Z. Phys. C – Particles and Fields 45, 11–23 (1989)

Zeitschrift für Physik C Particles and Fields

Experimental study of jet masses in e^+e^- annihilation at c.m. energies between 12 and 43.5 GeV

TASSO Collaboration

W. Braunschweig, R. Gerhards, F.J. Kirschfink [1], H.-U. Martyn
I. Physikalisches Institut der RWTH Aachen, D-5100 Aachen, Federal Republic of Germany [a]

H.M. Fischer, H. Hartmann, J. Hartmann, E. Hilger, A. Jocksch, R. Wedemeyer
Physikalisches Institut der Universität Bonn, D-5300 Bonn, Federal Republic of Germany [a]

B. Foster, A.J. Martin
H.H. Wills Physics Laboratory, University of Bristol, Bristol BS8 1TL, UK [b]

F. Barreiro [2], E. Bernardi [3], J. Chwastowski [4], K. Genser [5], H. Kowalski [6], B. Löhr, D. Lüke [7], D. Notz, J.M. Pawlak [5], K.-U. Pösnecker, E. Ros, R. Walczak [5], G. Wolf
Deutsches Elektronen-Synchrotron DESY, D-2000 Hamburg, Federal Republic of Germany

H. Kolanoski
Institut für Physik, Universität Dortmund, D-4600 Dortmund, Federal Republic of Germany

T. Kracht [8], J. Krüger, E. Lohrmann, G. Poelz, W. Zeuner [9]
II. Institut für Experimentalphysik der Universität Hamburg, D-2000 Hamburg, Federal Republic of Germany [a]

J. Hassard, J. Shulman, D. Su [10], I. Tomalin
Department of Physics, Imperial College, London SW7 2AZ, UK [b]

A. Leites [11], J. del Peso, L. Hervas, M. Traseira [11]
Universidad Autónoma de Madrid, 28049 Madrid, Spain [c]

M.G. Bowler, P.N. Burrows [12], R.J. Cashmore, G.P. Heath, M.E. Veitch
Department of Nuclear Physics, Oxford University, Oxford OX1 3RH, UK [b]

J.C. Hart, D.H. Saxon
Rutherford Appleton Laboratory, Chilton, Didcot, Oxon OX11 0QX, UK [b]

S. Brandt, M. Holder, L. Labarga [13]
Fachbereich Physik der Universität-Gesamthochschule Siegen, D-5900 Siegen, Federal Republic of Germany [a]

Y. Eisenberg, U. Karshon, G. Mikenberg, A. Montag, D. Revel, E. Ronat, A.N. Wainer, G. Yekutieli
Weizmann Institute, Rehovot 76100, Israel [d]

D. Muller [13], S. Ritz [14], M. Takashima [9], Sau Lan Wu, G. Zobernig, A. Caldwell [14]
Department of Physics, University of Wisconsin, Madison, WI 53706, USA [e]

Received 5 July 1989

[1] Now at Lufthansa, Hamburg, FRG
[2] Alexander von Humboldt Fellow, on leave of absence from Universidad Autónoma de Madrid
[3] Now at Robert Bosch GmbH, Schwieberdingen, FRG
[4] Now at Inst. of Nuclear Physics, Cracow, Poland
[5] Now at Warsaw University, Poland
[6] On leave at Columbia University, NY, USA
[7] On leave at CERN, Geneva, Switzerland
[8] Now at Hasylab, DESY
[9] Now at CERN, Geneva, Switzerland
[10] Now at Rutherford Appleton Laboratory, Chilton, UK
[11] Partially supported by DGICIT, Spain, and Kfz-Karlsruhe, FRG
[12] Now at MIT
[13] Now at SLAC, Standford, CA, USA
[14] Now at Columbia University, NY, USA

[a] Supported by Bundesministerium für Forschung und Technologie
[b] Supported by UK Science and Engineering Research Council
[c] Supported by CAICYT
[d] Supported by the Minerva Gesellschaft für Forschung GmbH
[e] Supported by US Dept. of Energy, contract DE-AC02-76ER000881 and by US Nat. Sci. Foundation Grant no INT-8313994 for travel

Abstract. Data on jet masses, resulting from the decomposition of e^+e^- hadronic final states into two hemispheres, are presented at centre of mass energies between 12 and 43.5 GeV. Comparisons are made with bare $O(\alpha_s^2)$ QCD predictions as well as with QCD based fragmentation models. Values for α_s and $\Lambda_{\overline{\text{MS}}}$ are determined, both with and without hadronization effects included. Upper and lower limits for $\Lambda_{\overline{\text{MS}}}$ independent of fragmentation models have been determined to be 0.480 ± 0.025 GeV and 0.047 ± 0.007 GeV respectively.

1 Introduction

Considerable efforts have been devoted in recent years to the study of multihadronic final states produced in e^+e^- annihilation. In order to test quantum chromodynamic usefully, the need to measure jet quantities which are only mildly sensitive to colour radiative corrections and to power corrections or fragmentation effects, has been stressed [1]. Jet masses were proposed long ago [2] for that purpose. Recently a systematic study of the properties exhibited by jet masses in perturbative QCD as well as the influence of fragmentation effects upon them, has been performed [3, 4]. In that study it was found useful to define the jet masses as follows:

- divide each event into two hemispheres using the plane perpendicular to the thrust axis [5]
- calculate the invariant mass of the particles in each hemisphere, denoting by $M_H(M_L)$ the heavier (lighter) of the two.

Cross sections $\frac{d\sigma}{dM^2/s}$, with $\frac{M^2}{s}=\frac{M_L^2}{s}, \frac{M_H^2}{s}, \frac{(M_H^2-M_L^2)}{s}$, were calculated in [3, 4] to $O(\alpha_s^2)$ using the ERT matrix elements [6]. The results for $\frac{M_H^2}{s}$ and $\frac{(M_H^2-M_L^2)}{s}$ can be written in the form:

$$\frac{1}{\sigma_T}\frac{d\sigma}{d\frac{M^2}{s}}=\frac{\alpha_s(Q^2)}{\pi}F\left(\frac{M^2}{s}\right)\left\{1+\frac{\alpha_s(Q^2)}{\pi}R\left(\frac{M^2}{s}\right)\right\} \quad (1)$$

where σ_T is the total cross-section to $O(\alpha_s^2)$ which in terms of the quark parton model cross-section σ_0 is given, in the $\overline{MS}$ scheme and for five flavours, by

$$\sigma_T=\sigma_0\left[1+\frac{\alpha_s(Q^2)}{\pi}+1.4\left(\frac{\alpha_s(Q^2)}{\pi}\right)^2\right] \quad (2)$$

$F\left(\frac{M^2}{s}\right)$ is a function calculated at $O(\alpha_s)$ [7] and $R\left(\frac{M^2}{s}\right)$ a function which measures the importance of second order corrections, roughly taking values:

$$R\left(\frac{M_H^2}{s}\right)\sim 10, \quad R\left(\frac{M_H^2-M_L^2}{s}\right)\sim 6.$$

These corrections lead to the following expansions for the mean values:

$$\left\langle\frac{M_H^2}{s}\right\rangle = 1.05\frac{\alpha_s}{\pi}+6.9\left(\frac{\alpha_s}{\pi}\right)^2$$
$$\left\langle\frac{M_H^2}{s}-\frac{M_L^2}{s}\right\rangle=1.05\frac{\alpha_s}{\pi}+2.9\left(\frac{\alpha_s}{\pi}\right)^2. \quad (3)$$

It is now generally accepted that the energy-energy correlation EEC and its corresponding asymmetry AEEC [8] are very powerful tools to test meaningfully low order perturbative QCD [1]. In a comparative QCD study presented in [3, 4] it was argued that since

$$R_{\text{EEC}}\sim 10, \quad R_{\text{AEEC}}\sim 3$$

both $\frac{M_H^2}{s}$ and $\frac{(M_H^2-M_L^2)}{s}$ are also quantities well suited to test low order perturbative QCD.

Notice that $\frac{M_L^2}{s}$ is to $O(\alpha_s)$ identically zero for massless quarks and gluons. It is therefore a quantity sensitive to higher order QCD and fragmentation effects.

In spite of the interesting properties discussed above, data on jet masses are meagre [9–11]. In particular, the energy variation of $\frac{M_H^2}{s}$, $\frac{M_L^2}{s}$ and $\frac{(M_H^2-M_L^2)}{s}$ is poorly measured. The purpose of this paper is twofold:

1. to present data on jet masses in a wide centre of mass energy range, namely 12–43.5 GeV, and
2. to make comparisons with bare QCD results, both with and without fragmentation effects included.

2 The data

The experiment was performed with the TASSO detector at PETRA. Details of the detector can be found elsewhere [12]. The data used for this analysis were taken in the period 1980–1986 at the centre of mass energies given in Table 1. Hadronic final states from

Table 1. Number of events and energy range of the data samples used in this analysis

$\sqrt{s}$ range (GeV)	$\langle\sqrt{s}\rangle$ (GeV)	No. of events
11.6–12.4	12.0	169
12.4–14.4	14.0	2530
21.0–23.0	22.0	1782
24.0–26.0	25.0	215
29.0–32.0	30.5	808
32.0–35.2	34.8	48558
35.2–38.4	37.5	2621
38.4–46.8	43.5	5913

e^+e^- annihilation were selected using the information on charged particle momenta measured in the central detector. The selection criteria for charged particles and for multihadron events are described in [13]. Basically, a charged track has to have a momentum component transverse to the beam of $p_{xy}>0.1$ GeV/c and a cosine of the polar angle of $|\cos\theta|<0.87$. The r.m.s. momentum resolution including multiple scattering is $\frac{\sigma_p}{p}=0.016(1+p^2)^{1/2}$, with p in GeV/c. The main criterion for multihadron events is based on the momentum sum of the accepted charged particles, $\sum_j p_j>0.265\sqrt{s}$.

Only charged particles were used in our analysis. To ensure a large acceptance for charged particles in jets we required $|\cos\theta_{tb}|<0.8$, where θ_{tb} is the angle between the event thrust axis and the beam direction.

As already discussed in the introduction, in order to measure the various jet masses, $\frac{M^2}{s}=\frac{M_H^2}{s}, \frac{M_L^2}{s}, \frac{(M_H^2-M_L^2)}{s}$, we start by determining the jet axis using a standard algorithm. The event is then partitioned into two hemispheres by the plane perpendicular to the jet axis. We then calculate the invariant masses squared of the particles in each of both hemispheres assigning them the pion mass. Finally these values are normalized to the visible charged energy squared.

The data distributions were corrected for initial state radiation and selection cuts bin by bin, and for neutral particles and detector effects with a probability matrix using standard Monte Carlo techniques [13]. For the sake of illustration we quote the total correction factors at $\sqrt{s}=43.5$ GeV, namely 1.0 ± 0.2 for $\frac{(M_H^2-M_L^2)}{s}$ and $\frac{M_H^2}{s}$ and 1.8 ± 0.2 for $\frac{M_L^2}{s}$ over most of the spectrum.

Systematic uncertainties in the correction procedure have been studied, in particular those coming from:

- cuts applied on the raw data
- differences in the fragmentation models used for calculating the correction factors
- the method used to divide the events into two hemispheres, either the plane perpendicular to the thrust or sphericity axis.

The largest contribution came from the second source. Four different models were considered for correction purposes, namely: the independent jet fragmentation model including $O(\alpha_s^2)$ corrections of Ali et al. [14], the string fragmentation model à la Lund including $O(\alpha_s^2)$ matrix elements [15], as well as two different parton shower models, i.e. the Lund [16] and Webber [17] models.

We then followed a procedure similar to that used by the MARK II Collaboration [9], i.e. we calculated a weighted average of the corrected distributions for $\frac{(M_H^2-M_L^2)}{s}$, $\frac{M_H^2}{s}$, and $\frac{M_L^2}{s}$ using the four fragmentation models mentioned above. The weights were chosen to be proportional to the probability of the various models considered fitting our raw jet masses data. Deviations from the average value [11] were taken as a measure of the systematic uncertainty in the correction procedure.

3 Comparison between data and Monte Carlo models

We show in Figs. 1, 2, 3 the corrected $\frac{M_L^2}{s}$, $\frac{M_H^2}{s}$ and $\frac{(M_H^2-M_L^2)}{s}$ distributions at $\sqrt{s}=14$, 22, 34.8, 43.5 GeV, together with the corresponding $O(\alpha_s^2)$ bare QCD calculations with $\Lambda_{\overline{\text{MS}}}=0.2$ GeV. The numerical values for these data are given in Tables 2, 3, 4. The errors quoted are the quadratic sums of statistical and systematic errors obtained following the prescription discussed in the preceding section.

The three quantities show a similar trend with increasing centre of mass energy, namely the distributions become narrower and the position of the peaks shift to lower values of the variables $\frac{M^2}{s}$. Notice that while the experimental distributions are normalized to unit area, the theoretical curves are normalized in such a way that their integral gives the sum of three- and four-jet cross-section as a fraction of the total cross section. One might then expect data and bare QCD predictions to converge, at high enough energies, in the so called perturbative tail, where the contribution from two jets is expected to be smallest [3, 4].

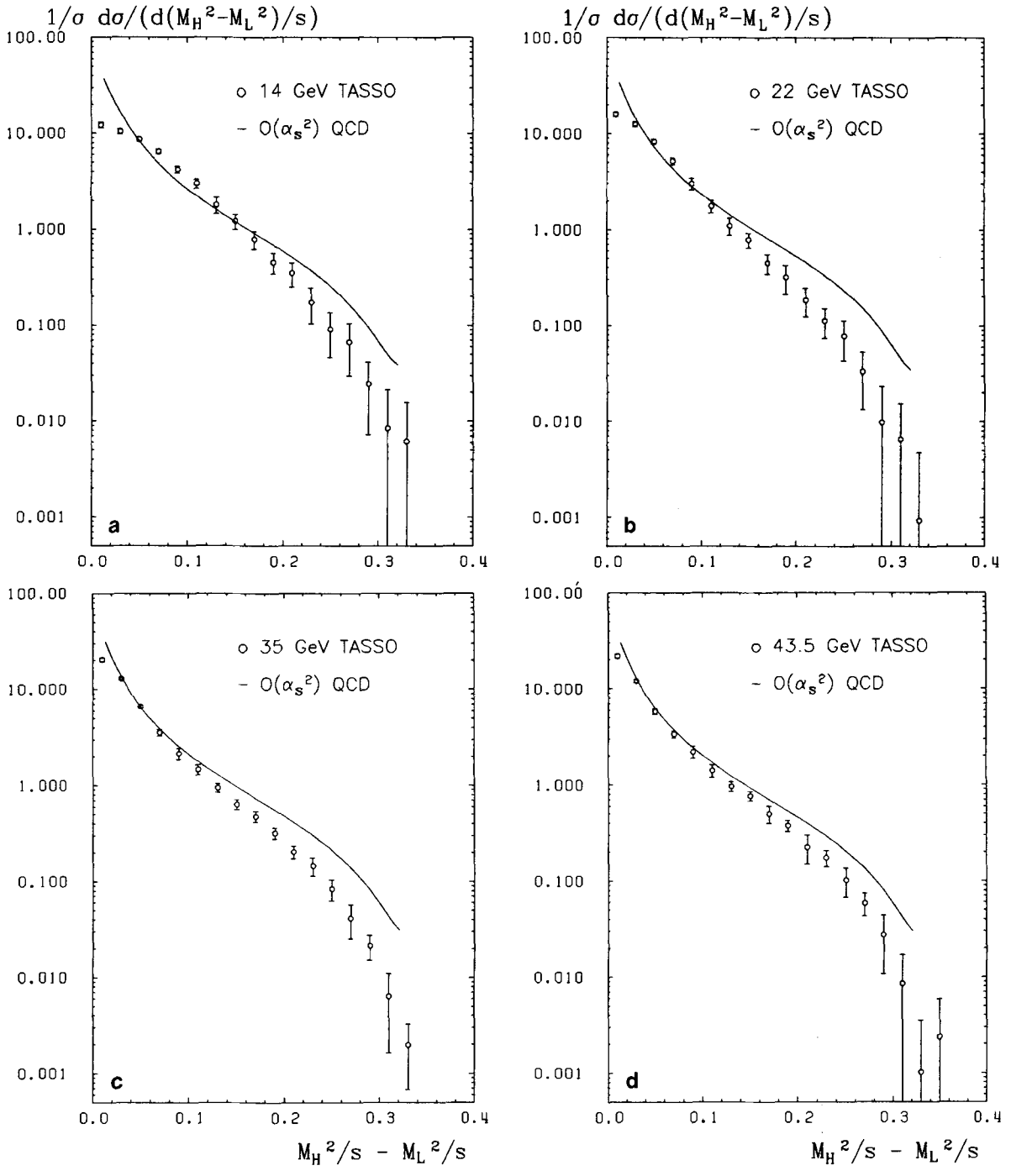

Fig. 1a–d. $\frac{(M_H^2 - M_L^2)}{s}$ data distributions for $\sqrt{s} = 14$, 22, 35 and 43.5 GeV and comparison with $O(\alpha_s^2)$ QCD for $\Lambda_{\overline{MS}} = 0.2$ GeV

In fact, we observe that the experimental distributions tend to approach the bare QCD predictions as the c.m. energy increases. However, even at the highest energies the experimental cross-section for the light jet mass is off by a large factor (5–10) with respect to the $O(\alpha_s^2)$ QCD calculation.

As discussed in detail in [3, 4] the light jet mass receives non-zero contributions in perturbative QCD only beyond $O(\alpha_s)$. Indeed, higher order effects as estimated with the help of a parton shower model [17] are found to be very large. We consider that this is an important reason for the large discrepancy be-

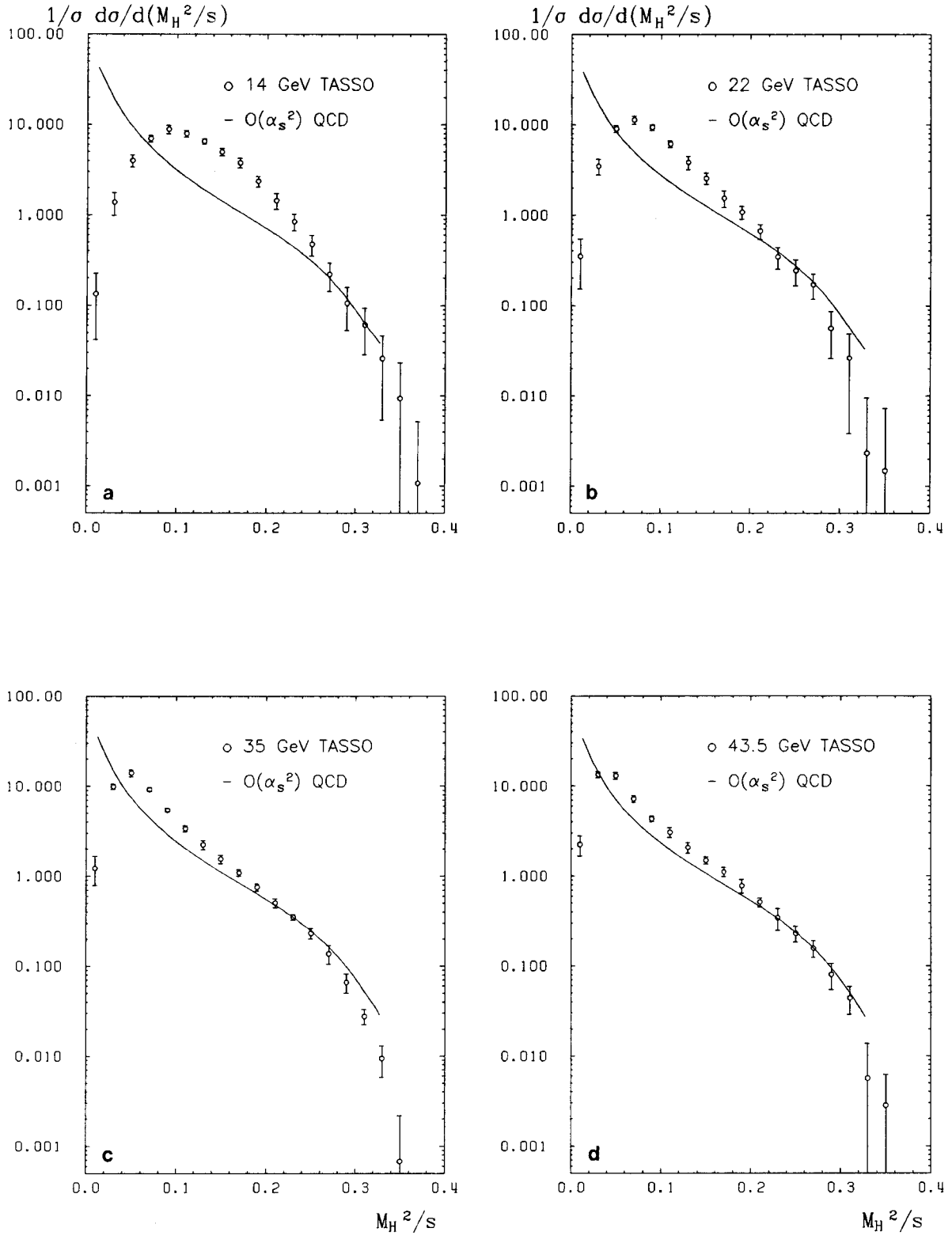

Fig. 2a–d. $\frac{M_H^2}{s}$ data distributions for $\sqrt{s}=14$, 22, 35 and 43.5 GeV and comparison with $O(\alpha_s^2)$ QCD for $\Lambda_{\overline{\text{MS}}}=0.2$ GeV

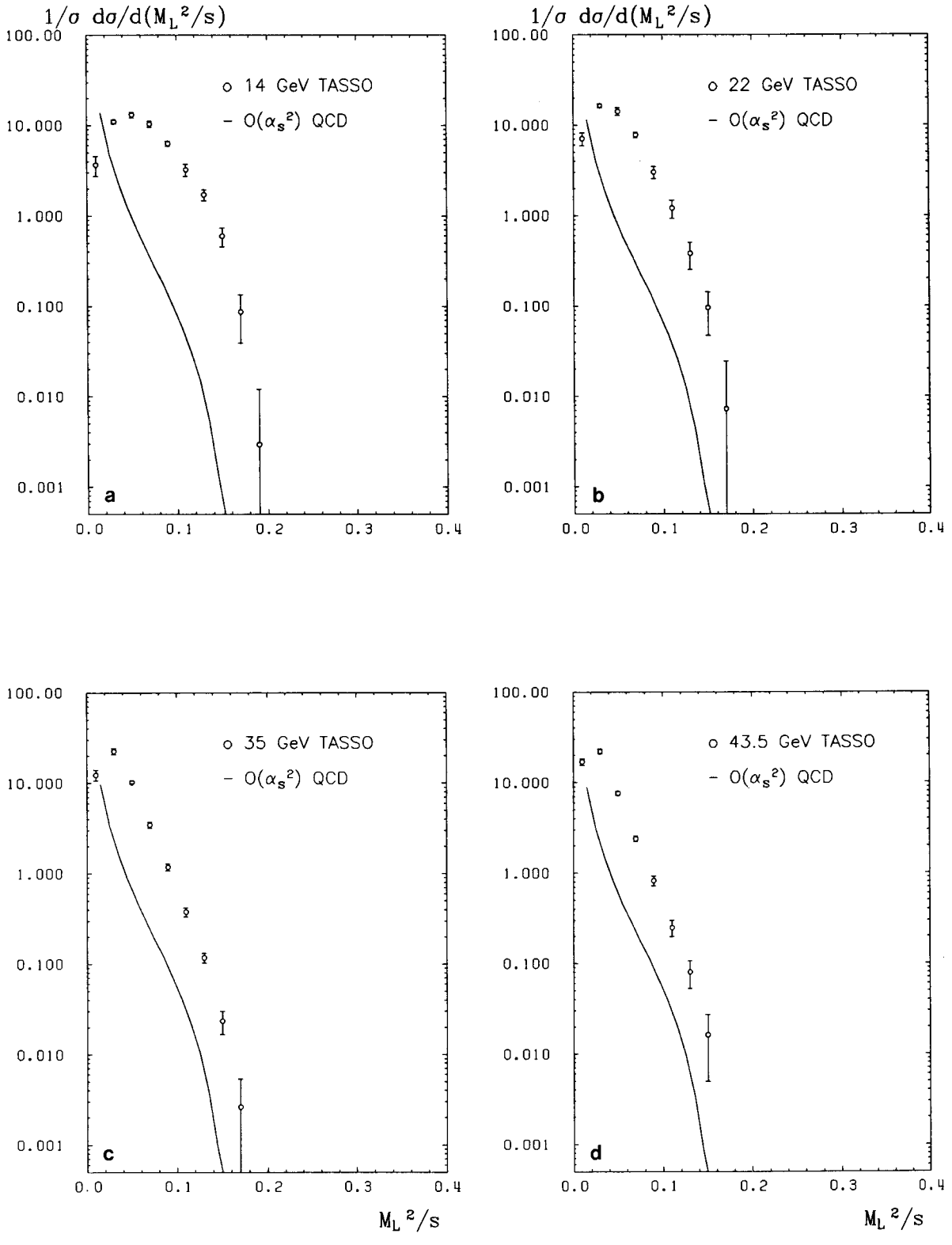

Fig. 3a–d. $\frac{M_L^2}{s}$ data distributions for $\sqrt{s}=14$, 22, 35 and 43.5 GeV and comparison with $O(\alpha_s^2)$ QCD for $\Lambda_{\overline{\text{MS}}}=0.2$ GeV

Table 2. Differential cross sections $\frac{1}{\sigma}\frac{d\sigma}{d(M_H^2-M_L^2)/s}$ at four centre of mass energies

$(M_H^2-M_L^2)/s$	$\sqrt{s}=14.0$ GeV	$\sqrt{s}=22.0$ GeV	$\sqrt{s}=34.8$ GeV	$\sqrt{s}=43.5$ GeV
0.00–0.02	12.25 ±0.81	15.98 ±0.84	20.35 ±0.93	21.9 ±1.1
0.02–0.04	10.44 ±0.64	12.64 ±0.68	12.93 ±0.32	12.06 ±0.47
0.04–0.06	8.65 ±0.47	8.26 ±0.47	6.64 ±0.20	5.85 ±0.40
0.06–0.08	6.43 ±0.37	5.19 ±0.43	3.57 ±0.27	3.37 ±0.28
0.08–0.10	4.19 ±0.32	3.00 ±0.42	2.15 ±0.29	2.19 ±0.31
0.10–0.12	3.00 ±0.32	1.77 ±0.28	1.47 ±0.18	1.41 ±0.21
0.12–0.14	1.81 ±0.35	1.10 ±0.22	0.95 ±0.10	0.96 ±0.11
0.14–0.16	1.22 ±0.22	0.78 ±0.13	0.635±0.074	0.762±0.085
0.16–0.18	0.78 ±0.16	0.45 ±0.11	0.476±0.062	0.50 ±0.10
0.18–0.20	0.45 ±0.11	0.32 ±0.10	0.320±0.043	0.374±0.051
0.20–0.22	0.35 ±0.10	0.184±0.060	0.203±0.031	0.223±0.074
0.22–0.24	0.174±0.070	0.112±0.038	0.146±0.031	0.173±0.033
0.24–0.26	0.091±0.044	0.078±0.035	0.083±0.020	0.102±0.034
0.26–0.28	0.067±0.037	0.033±0.020	0.041±0.016	0.058±0.016
0.28–0.30	0.024±0.017	–	0.021±0.003	0.027±0.017
0.30–0.32	–	–	0.006±0.005	0.009±0.009
0.32–0.34	–	–	0.002±0.001	–

Table 3. Differential cross sections $\frac{1}{\sigma}\frac{d\sigma}{dM_H^2/s}$ at four centre of mass energies

M_H^2/s	$\sqrt{s}=14.0$ GeV	$\sqrt{s}=22.0$ GeV	$\sqrt{s}=34.8$ GeV	$\sqrt{s}=43.5$ GeV
0.00–0.02	0.13 ±0.09	0.35 ±0.20	1.22 ±0.44	2.23 ±0.57
0.02–0.04	1.38 ±0.38	3.46 ±0.68	9.89 ±0.64	13.35 ±1.05
0.04–0.06	3.98 ±0.61	9.00 ±0.81	13.96 ±1.18	12.96 ±1.18
0.06–0.08	7.01 ±0.58	11.23 ±1.15	9.19 ±0.43	7.19 ±0.62
0.08–0.10	8.84 ±0.97	9.32 ±0.67	5.43 ±0.22	4.30 ±0.32
0.10–0.12	7.90 ±0.66	6.12 ±0.52	3.39 ±0.27	3.04 ±0.37
0.12–0.14	6.51 ±0.43	3.82 ±0.64	2.24 ±0.25	2.06 ±0.28
0.14–0.16	4.96 ±0.46	2.55 ±0.36	1.55 ±0.17	1.49 ±0.14
0.16–0.18	3.77 ±0.45	1.53 ±0.32	1.088±0.088	1.11 ±0.13
0.18–0.20	2.35 ±0.31	1.07 ±0.17	0.752±0.071	0.78 ±0.14
0.20–0.22	1.44 ±0.29	0.66 ±0.13	0.505±0.056	0.551±0.058
0.22–0.24	0.84 ±0.17	0.344±0.092	0.351±0.025	0.342±0.093
0.24–0.26	0.47 ±0.12	0.242±0.078	0.233±0.031	0.230±0.045
0.26–0.28	0.219±0.076	0.170±0.052	0.137±0.032	0.156±0.033
0.28–0.30	0.106±0.053	0.056±0.030	0.066±0.016	0.080±0.026
0.30–0.32	0.061±0.033	0.026±0.022	0.028±0.005	0.044±0.015
0.32–0.34	0.026±0.020	–	0.009±0.004	–

Table 4. Differential cross sections $\frac{1}{\sigma}\frac{d\sigma}{dM_L^2/s}$ at four centre of mass energies

M_L^2/s	$\sqrt{s}=14.0$ GeV	$\sqrt{s}=22.0$ GeV	$\sqrt{s}=34.8$ GeV	$\sqrt{s}=43.5$ GeV
0.00–0.02	3.66 ±0.92	7.04 ±1.14	12.28 ±1.62	16.88 ±1.38
0.02–0.04	11.00 ±0.59	16.42 ±0.77	22.41 ±1.67	22.00 ±1.33
0.04–0.06	13.07 ±0.95	14.20 ±1.33	10.23 ±0.43	7.58 ±0.38
0.06–0.08	10.40 ±0.80	7.77 ±0.51	3.45 ±0.26	2.38 ±0.17
0.08–0.10	6.30 ±0.40	3.02 ±0.46	1.18 ±0.11	0.82 ±0.10
0.10–0.12	3.24 ±0.50	1.21 ±0.28	0.38 ±0.042	0.248±0.050
0.12–0.14	1.72 ±0.24	0.38 ±0.13	0.12 ±0.015	0.080±0.027
0.14–0.16	0.60 ±0.14	0.096±0.048	0.024±0.007	0.016±0.011
0.16–0.18	0.087±0.048	–	–	–

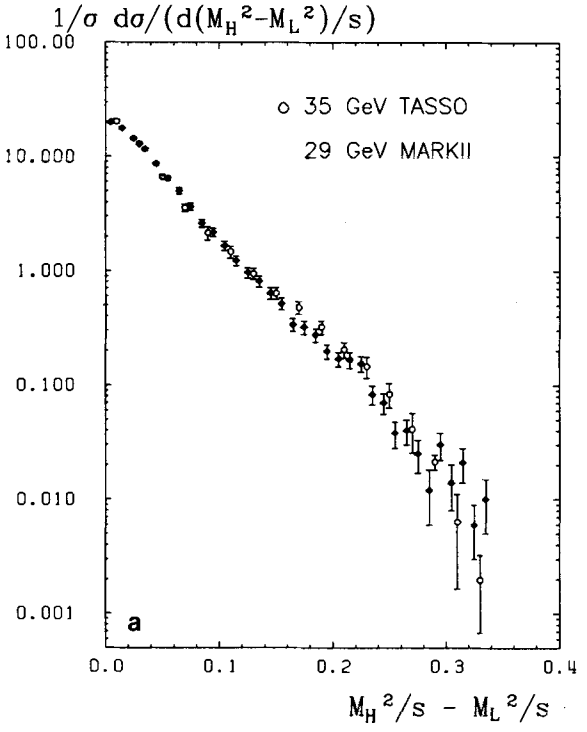

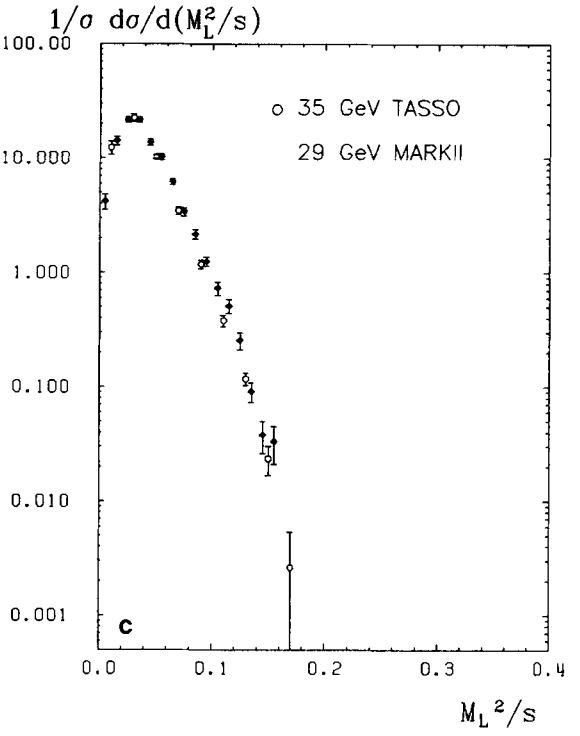

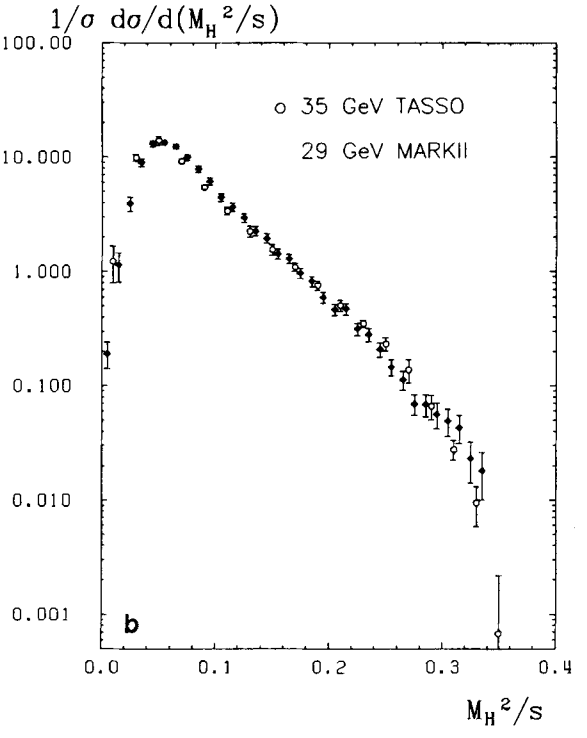

Fig. 4a–c. Comparison of the data distributions of TASSO at 35 GeV and MARK II at 29 GeV

tween data and bare QCD predictions for the light jet mass, as well as for the much milder disagreements between the experimental distributions for the jet mass difference and the $O(\alpha_s^2)$ bare QCD predictions.

For the sake of completeness we show in Fig. 4 the $\frac{(M_H^2-M_L^2)}{s}, \frac{M_H^2}{s}, \frac{M_L^2}{s}$ distributions for the 29 GeV MARK II data [9] and the 34.8 GeV TASSO data. The agreement is very good, despite the fact that the energies are slightly different.

In order to describe the experimental distribution for $\frac{M_H^2}{s}$, $\frac{M_L^2}{s}$ and $\frac{(M_H^2-M_L^2)}{s}$, over their whole range of variation, we need to convolute the bare QCD predictions to $O(\alpha_s^2)$ with model dependent fragmentation schemes for quarks and gluons. We will consider two rather different fragmentation pictures, the independent jet fragmentation model by Ali et al. (IJF) [14] and the Lund model (Lund) [15]. The model parameter values were taken from [11], [18]. In Fig. 5 we present a comparison between our data at the highest energy, $\sqrt{s}=43.5$ GeV, where the influence of fragmentation effects is relatively smaller, and the results of fits using the models of [14] and [15]. The agreement between data and both models is satisfactory. Values obtained for α_s and the QCD scale $\Lambda_{\overline{\text{MS}}}$ are given in Table 5. The systematic errors are a quadratic sum of those coming from the correction proce-

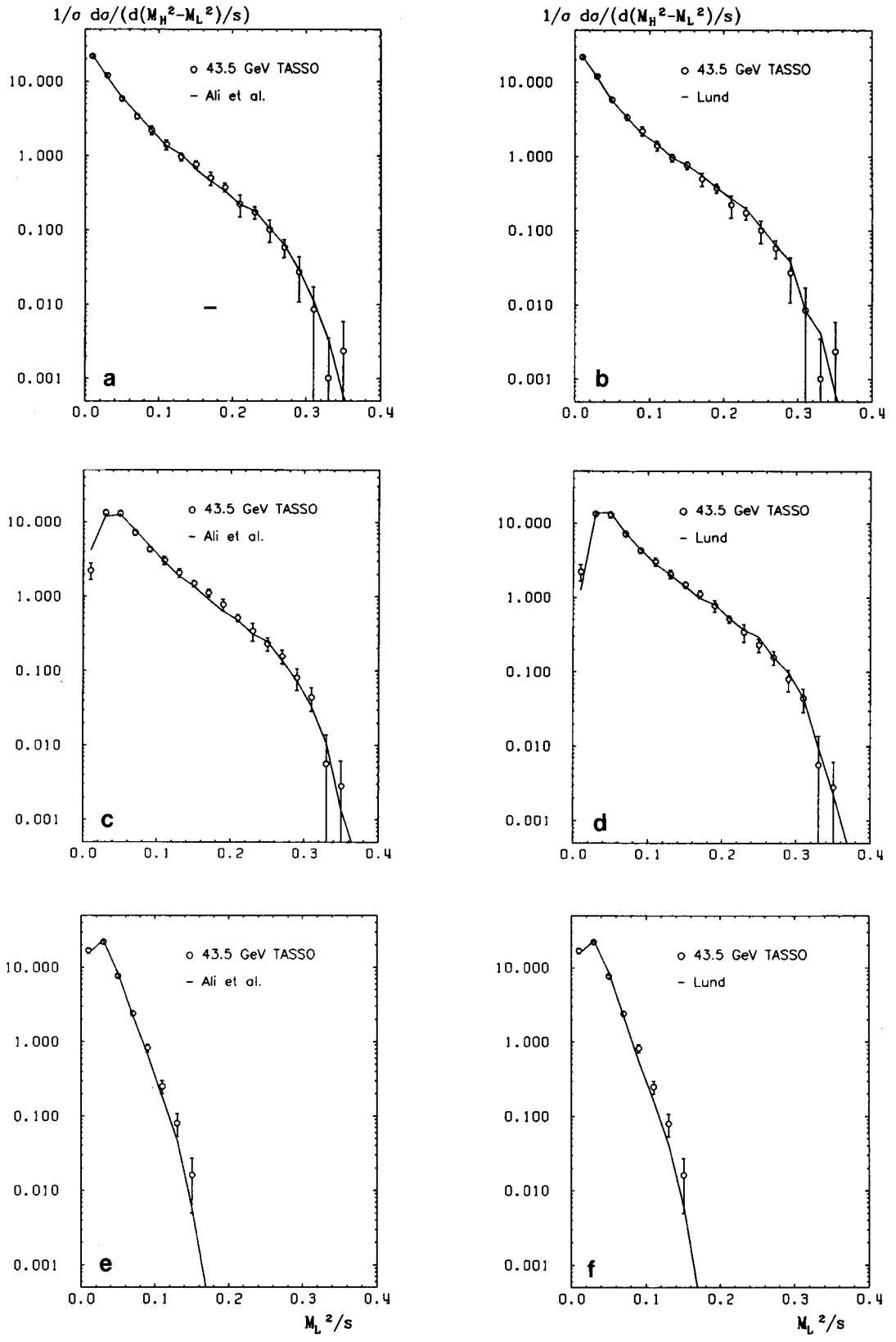

Fig. 5a–c. Fits of the IJF and Lund models incorporating exact $O(\alpha_s^2)$ QCD matrix elements to the $\frac{(M_H^2-M_L^2)}{s}$, $\frac{M_H^2}{s}$ and $\frac{M_L^2}{s}$ data distributions at 43.5 GeV

Table 5. Values of α_s from fits to the jet mass data distributions at 43.5 GeV, using the independent jet fragmentation model (IJF) and the Lund model with exact $O(\alpha_s^2)$ corrections. The systematic errors quoted come from the correction procedure and the choice of fragmentation parameters

Model	Measure	α_s(43.5 GeV)	$\Lambda_{\overline{\text{MS}}}$(GeV)
IJF	$\frac{M_H^2}{s}-\frac{M_L^2}{s}$	$0.120\pm0.002\pm0.007$	$0.100\pm0.012\pm0.030$
IJF	$\frac{M_H^2}{s}$	$0.134\pm0.002\pm0.007$	$0.210\pm0.014\pm0.055$
Lund	$\frac{M_H^2}{s}-\frac{M_L^2}{s}$	$0.147\pm0.003\pm0.009$	$0.340\pm0.032\pm0.100$
Lund	$\frac{M_H^2}{s}$	$0.158\pm0.002\pm0.009$	$0.500\pm0.024\pm0.135$

dure (2%–3%) and those coming from the dependence on the fragmentation parameters (5%–6%). We do not use the light jet mass to determine α_s, because it is a quantity very sensitive to hadronization fluctuations.

The values for α_s shown in Table 5 exhibit uncertainties similar to those affecting other jet measures like the AEEC. As is well known, different fragmentation schemes give rather different values of α_s. The systematic errors quoted in Table 5 do not reflect this model dependence. For this reason in the next section we will extract model independent limits of α_s and $\Lambda_{\overline{\text{MS}}}$.

An estimate of the importance of the fragmentation term can be obtained from the quantity:

$$\Delta\left(\frac{M^2}{s}\right)=\frac{\left.\frac{1}{\sigma}\frac{d\sigma}{dM^2/S}\right|_{\text{FR}}-\left.\frac{1}{\sigma_T}\frac{d\sigma}{dM^2/S}\right|_{\text{QCD}}}{\left.\frac{1}{\sigma_T}\frac{d\sigma}{dM^2/S}\right|_{\text{QCD}}} \tag{4}$$

where the subscripts QCD and FR denote parton ($O(\alpha_s^2)$) and hadron level respectively.

Using both the independent jet fragmentation and the Lund models, it has been shown [3, 4] that

- $\Delta(M^2/s)$ decreases as $\sqrt{s}$ increases
- $\Delta((M_H^2/s)$ strongly decreases when M_H^2/s increases, i.e. becomes small when at high energies ($\sqrt{s}>20$ GeV) one approaches the perturbative tail $\left(\frac{M_H^2}{s}>0.2\right)$
- $\Delta((_H^2-M_L^2)/s)$ is negative and non-negligible even at our highest energies.

4 The energy behaviour of jet masses

In order to have a closer look at the energy behaviour of the jet masses, we plot in Fig. 6 the integrated cross sections $\int_a^b \frac{1}{\sigma}\frac{d\sigma}{d(M^2/s)}d\left(\frac{M^2}{s}\right)$, for $\frac{M^2}{s}=\frac{M_H^2}{s}$,

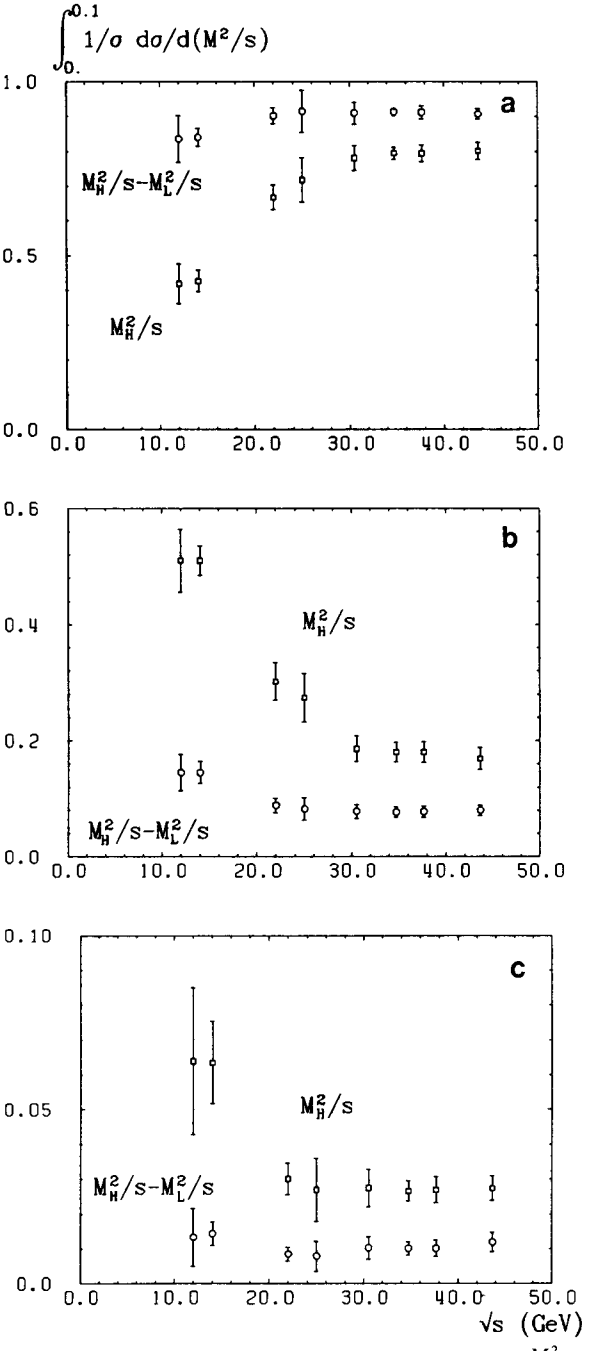

Fig. 6a–c. Integrated cross section for data in the region **a** $\frac{M^2}{s}<0.1$; **b** $0.1<\frac{M^2}{s}<0.2$; **c** $\frac{M^2}{s}>0.2$ of the jet mass difference and the heavy jet mass as a function of the c.m. energy

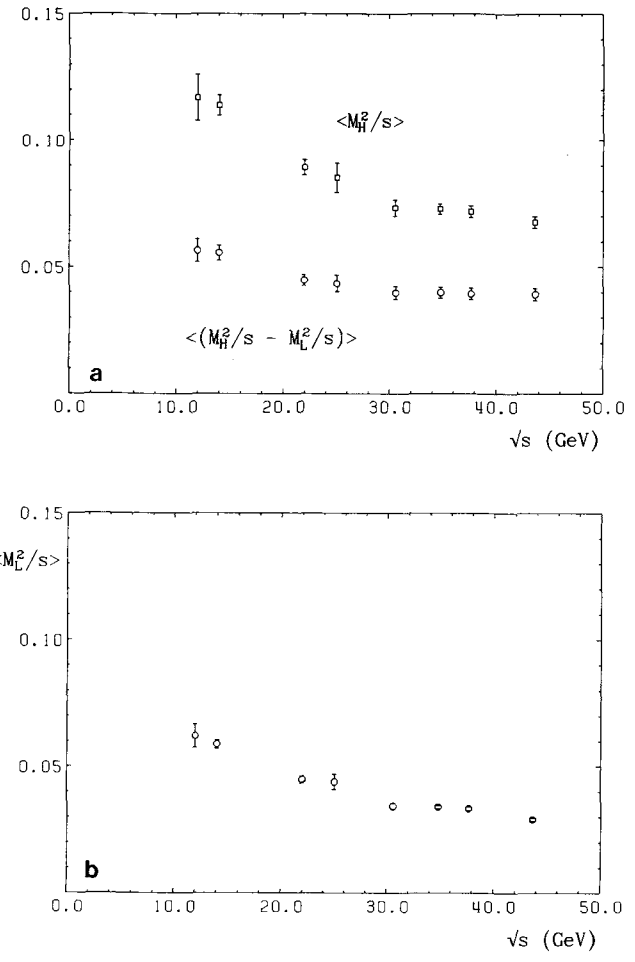

Fig. 7a, b. Mean values **a** $\left\langle \frac{M_H^2}{s} \right\rangle$ and $\left\langle \frac{(M_H^2 - M_L^2)}{s} \right\rangle$; **b** $\left\langle \frac{M_L^2}{s} \right\rangle$ for data as a function of the c.m. energy

$\frac{(M_H^2 - M_L^2)}{s}$ over three regions of the spectrum, namely $\left(0.0 < \frac{M^2}{s} < 0.1\right)$, $\left(0.1 < \frac{M^2}{s} < 0.2\right)$ and $\left(0.2 < \frac{M^2}{s}\right)$, as a function of the centre of mass energy. The data show a rather strong energy variation for the small c.m. energies. This is due to fragmentation effects. At higher c.m. energies, where fragmentation effects become smaller, the data tend to flatten off as one would expect for the logarithmic energy dependence implicit in (1) through the energy variation of α_s. The onset of this flattening off takes place at smaller c.m. energies for the highest $\frac{M^2}{s}$ region.

For the sake of completeness we also show in Fig. 7 the mean values $\left\langle \frac{M_H^2}{s} \right\rangle$, $\left\langle \frac{(M_H^2 - M_L^2)}{s} \right\rangle$ and $\left\langle \frac{M_L^2}{s} \right\rangle$ as a function of the centre of mass energy. These data

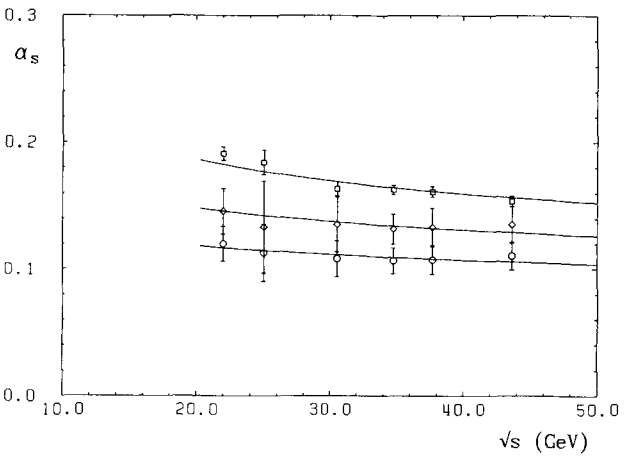

Fig. 8. Energy dependence of α_s calculated applying Eq. 3 to data on $\left\langle \frac{M_H^2}{s} \right\rangle$ (squares) and applying (5) with $\Delta\left(\frac{M^2}{s}\right) = 0$ to the heavy jet mass over the region $\frac{M_H^2}{s} > 0.2$ (diamonds) and to the jet mass difference over the region $0.1 < \frac{(M_H^2 - M_L^2)}{s} < 0.2$ (circles). The full lines correspond to the $O(\alpha_s^2)$ QCD dependence for $\Lambda_{\overline{\text{MS}}} = 0.480$ GeV (upper curve) $\Lambda_{\overline{\text{MS}}} = 0.170$ GeV (middle curve) and $\Lambda_{\overline{\text{MS}}} = 0.045$ GeV (lower curve)

exhibit a behaviour similar to that discussed above for the integrated cross sections.

These observations on the importance of fragmentation effects to the measured energy behaviour of the jet masses agree with the discussion in the previous section.

If we naively assume that the cross sections can be expressed as the sum of the perturbative contribution to $O(\alpha_s^2)$ plus a fragmentation term [10, 19], we can write

$$\int_a^b \frac{\alpha_s(Q^2)}{\pi} F\left(\frac{M^2}{s}\right)\left(1 + \frac{\alpha_s(Q^2)}{\pi} R\left(\frac{M^2}{s}\right)\right) \cdot \left(1 + \Delta\left(\frac{M^2}{s}\right)\right) d\left(\frac{M^2}{s}\right) = \int_a^b \frac{1}{\sigma} \frac{d\sigma^{\text{exp}}}{d\frac{M^2}{s}} d\left(\frac{M^2}{s}\right) \qquad (5)$$

with $\frac{M^2}{s} = \frac{M_H^2}{s}, \frac{(M_H^2 - M_L^2)}{s}$.

By going to a region where fragmentation effects are small, we can derive approximate values for α_s in a model independent way from (5) by setting $\Delta\left(\frac{M^2}{s}\right)$ equal to zero. Values of α_s, for $\sqrt{s} > 20$ GeV, obtained when applying (5) to the integrated cross sections in such a region, where fragmentation effects are small, namely $\frac{M_H^2}{s} > 0.2$, are shown as the diamonds in Fig. 8. The line is the result of a fit using

the α_s energy variation:

$$\alpha_s(Q^2)=\frac{2\pi}{\frac{1}{6}(33-2N_f)\ln\left(\frac{Q^2}{\Lambda^2}\right)+\frac{(153-19N_f)}{(33-2N_f)}\ln\ln\left(\frac{Q^2}{\Lambda^2}\right)} \quad (6)$$

obtaining $\Lambda_{\overline{\rm MS}}=0.170\pm0.047$ GeV. If we only look at the highest energy point, $\sqrt{s}=43.5$ GeV, where fragmentation effects are the smallest*, we obtain the α_1 value, $\alpha_s=0.135\pm0.014$.

In those regions where fragmentation effects are not small, the values of α_s, estimated when using (5) with $\Delta\left(\frac{M^2}{s}\right)=0$, can be considered as upper or lower limits depending on whether the fragmentation term is positive or negative respectively. An example of such a region is $0.1<\frac{(M_H^2-M_L^2)}{s}<0.2$ for energies above 20 GeV. We parametrise the energy dependence in Fig. 6b by the sum [10]

$$(a_1\,\alpha_s/\pi)(1+a_2\,\alpha_s/\pi)+\frac{b}{\sqrt{s}}$$

where a_1 and a_2 are the integrals over the region $0.1<\frac{(M_H^2-M_L^2)}{s}<0.2$ of $F\left(\frac{M_H^2-M_L^2}{s}\right)$ and $R\left(\frac{M_H^2-M_L^2}{s}\right)$ respectively and $\frac{b}{\sqrt{s}}$ represents the energy variation of the fragmentation term as given in a limited p_t parton model. Fitting the above formula to our data for all $\Lambda_{\overline{\rm MS}}$ values greater than 0.045 GeV results in $b<0$. This points to the fact that the fragmentation term is indeed negative as was found from Monte Carlo calculations in [3, 4]. Values of α_s for $\sqrt{s}>20$ GeV obtained from the jet mass difference data displayed in Fig. 6b are presented as open circles in Fig. 8. The lower line corresponds to a fit using as the α_s energy variation the expression given above (6). From that fit we obtain the value $\Lambda_{\overline{\rm MS}}=0.045\pm0.016$ GeV. By using as before only the highest energy point, we obtain α_s (43.5 GeV) $=0.110\pm0.011$, which can therefore be considered as a lower limit.

An alternative way to extract limits to α_s is to use (3) to fit the data of Fig. 7a. Again, if the neglected fragmentation term is positive or negative, an upper or lower limit respectively would come out. It is clearly seen from Fig. 2 that the heavy jet mass experimental distributions peak at higher values than the perturbative QCD predictions. This indicates that the fragmentation contribution to $\left\langle\frac{M_H^2}{s}\right\rangle$ is positive. An explicit Monte Carlo calculation using both IJF and Lund models corroborates our expectation [4]. Values of α_s obtained when applying (3) to desribe our data on $\left\langle\frac{M_H^2}{s}\right\rangle$ are represented in Fig. 8 as squares. According to the previous discussion these values should be considered as upper limits. At the highest energy we obtain α_s (43.5 GeV) $=0.153\pm0.004$. Also plotted is the result of a fit for energies above 20 GeV using the α_s energy variation given by (6). From that fit we obtain the value $\Lambda_{\overline{\rm MS}}=0.480\pm0.025$ GeV. The Monte Carlo calculations with the IJF and Lund models also show that $\left\langle\frac{(M_H^2-M_L^2)}{s}\right\rangle$ receives a negative fragmentation contribution, at least for $\sqrt{s}>20$ GeV. This indicates that values of α_s obtained when applying (3) to describe the data of Fig. 7a are indeed lower limits. The point at 43.5 GeV leads to the value $\alpha_s=0.107\pm0.006$, while the energy variation from 22 to 43.5 GeV gives $\Lambda_{\overline{\rm MS}}=0.047\pm0.007$ GeV.

We would like to point out that these upper and lower limits are in agreement with those extracted by other experiments using a similar technique [10, 19, 20].

5 Summary

We have presented data on heavy and light jet masses, $\frac{M_H^2}{s}$, $\frac{M_L^2}{s}$, as well as their difference, $\frac{(M_H^2-M_L^2)}{s}$, in the range of centre of mass energies from 12 GeV to 43.5 GeV. We observe that the experimental distributions for heavy jet masses as well as for jet mass differences approach the bare QCD predictions when the energy increases. The differential cross section as a function of light jet mass is very much greater than the corresponding low order QCD predictions at all centre of mass energies which we have studied, as expected.

Convoluting the $O(\alpha_s^2)$ bare QCD prediction either with the Ali et al. independent jet fragmentation or with Lund fragmentation, we obtained a reasonable description of our data across the whole mass spectrum. Values of α_s obtained with these models are in the range of those obtained with other jet measures [21, 22].

By using $O(\alpha_s^2)$ bare QCD to describe the energy variation of the $\frac{M_H^2}{s}$ cross section above 0.2, where

* According to Monte Carlo calculations performed in [3, 4] those fragmentation effects are ~5% for IJF and ~15% for Lund

fragmentation effects are expected to be small, we have determined the QCD scale parameter, to be $\Lambda_{\overline{\rm MS}} = 0.170 \pm 0.047$ GeV (corresponding to $\alpha_s = 0.129 \pm 0.006$ at $\sqrt{s} = 43.5$ GeV). This determination is very nicely bracketed between model independent upper and lower limits for $\Lambda_{\overline{\rm MS}}$ obtained using the energy variation of $\left\langle \frac{M_H^2}{s} \right\rangle$ and $\left\langle \frac{(M_H^2 - M_L^2)}{s} \right\rangle$. These values are: 0.480 ± 0.025 GeV and 0.047 ± 0.007 GeV respectively (corresponding to $\alpha_s = 0.157 \pm 0.002$ and $\alpha_s = 0.107 \pm 0.002$ at $\sqrt{s} = 43.5$ GeV).

Acknowledgements. We gratefully acknowledge the support of the DESY directorate, the PETRA machine group and the DESY computer centre. Those of us from outside DESY wish to thank the DESY directorate for the hospitality extended to us while working at DESY.

References

1. F. Barreiro: Fortschr. Phys. 34 (1986) 503; A. Ali, F. Barreiro: High energy e^+e^- annihilations. A. Ali, Pl. Söding (eds.), p. 612 Singapore: World Scientific
2. L. Clavelli: Phys. Lett. 85B (1979) 111; T. Chandramohan, L. Clavelli: Phys. Lett. 94B (1980) 409; L. Clavelli, D. Wyler: Phys. Lett. 103B (1981) 383
3. J. del Peso, L. Labarga, F. Barreiro: Z. Phys. C – Particles and Fields 43 (1985) 287
4. J. del Peso: Ph.D. Thesis, Universidad Autónoma de Madrid, FTUAM-EP-89-02 (1989)
5. S. Brandt, Ch. Peyrou, R. Sosnowski, A. Wroblewski: Phys. Lett. 12 (1964) 57
6. R.K. Ellis, D.A. Ross, A.E. Terrano: Phys. Rev. Lett. 45 (1980) 1226; Nucl. Phys. B178 (1981) 421
7. A. de Rujula, J. Ellis, E.G. Floratos, M.K. Gaillard: Nucl. Phys. B138 (1978) 387
8. C. Basham, L. Brown, S. Ellis, S. Love: Phys. Rev. Lett. 41 (1978) 1585; Phys. Rev. D19 (1979) 2018; Phys. Rev. D24 (1981) 2382
9. MARK II Coll. A. Petersen et al.: Phys. Rev. D37 (1988) 1
10. PLUTO Coll. Ch. Berger et al.: Z. Phys. C – Particles and Fields 12 (1982) 297
11. TASSO Coll. W. Braunschweig et al.: Z. Phys. C – Particles and Fields 41 (1988) 359
12. TASSO Coll. R. Brandelik et al.: Phys. Lett. 83B (1979) 261; Z. Phys. C – Particles and Fields 4 (1980) 87
13. TASSO Coll. M. Althoff et al.: Z. Phys. C – Particles and Fields 22 (1984) 307
14. A. Ali et al.: Phys. Lett B93 (1980) 155; Nucl. Phys. B168 (1980) 409
15. T. Sjöstrand: Comp. Phys. Commun. 39 (1986) 347; B. Andersson, G. Gustafson, G. Ingelman, T. Sjöstrand: Phys. Rep. 97 (1983) 33
16. M. Bengtsson, T. Sjöstrand: Phys. Lett. B185 (1987) 435
17. G. Marchesini, B.R. Webber: Nucl. Phys. B238 (1984) 1; B.R. Webber: Nucl. Phys. B238 (1984) 492
18. TASSO Coll. M. Althoff et al.: Z. Phys. C – Particles and Fields 26 (1984) 157
19. R.D. Field: Proceedings of the 1983 International Conference on Lepton-Photon Interactions, Cornell University, p. 593
20. CELLO Coll. H.J. Behrend et al.: DESY 89–19 (1989)
21. TASSO Coll. W. Braunschweig et al.: Z. Phys. C – Particles and Fields 36 (1987) 349; L. Labarga: Ph.D. Thesis, Universidad Autónoma de Madrid, unpublished (1987)
22. S.L. Wu: Rapporteur talk at the International Conference on Lepton-Photon Interactions, Hamburg 1987, W. Bartel, R. Rückl (eds.) p. 39. Amsterdam: B. Naroska: Phys. Rep. 148 (1987) 67; W.J. Stirling, M.R. Whalley: RAL-87-107 (1987), for a recent data compilation